

## Off-Axis Imaging Properties of Substrate Lens Antennas

Daniel F. Filipovic, George V. Eleftheriades and Gabriel M. Rebeiz

NASA/Center for Space Terahertz Technology  
Electrical Engineering and Computer Science Department  
University of Michigan  
Ann Arbor, MI 48109-2122

### ABSTRACT

In this paper, the theoretical far-field patterns and Gaussian-beam coupling efficiencies are investigated for a double-slot antenna placed off-axis on extended hemispherical silicon and quartz lenses. Measured off-axis radiation patterns at 258GHz agree well with the theory. Results are presented which show all important parameters versus off-axis displacement: scan angle, directivity, Gaussicity, and reflection loss. Directivity contour plots are also presented which show that near diffraction-limited performance can be achieved at off-axis positions at non-elliptical extension lengths.

### I. INTRODUCTION

A convenient method to eliminate substrate modes with integrated antennas is to place the antenna on a substrate lens. If the substrate lens has the same dielectric constant as the planar antenna wafer, then substrate modes will not exist. In addition, antennas placed on substrate lenses tend to radiate most of their power into the lens side, making the pattern unidirectional on high dielectric constant lenses. The ratio of powers between the dielectric and air is approximately  $\epsilon_r^{3/2}$  for slot and dipole-type antennas, where  $\epsilon_r$  is the relative dielectric constant of the lens. The substrate lens is an attractive solution for millimeter-wave antennas, since it also provides mechanical rigidity and thermal stability.

Previous investigations [1,2,3,4] have shown that the directivity of the substrate lens can be controlled by increasing or decreasing the extension length. In particular, as the extension length increases from the hyperhemispherical length ( $R/n$ , where  $R$  is the radius and

$n$  is the index of refraction of the lens), the directivity increases until it reaches a maximum diffraction-limited value. At the extension length which realizes maximum directivity, the extended hemispherical lens has a surface which approximates an elliptical lens, with the planar antenna at the more distant focus.

While the directivity increases at higher extension lengths, the pattern-to-pattern coupling value to a fundamental Gaussian-beam (Gaussicity) decreases [1]. Since the double-slot feed antenna used in these studies launches a nearly perfect fundamental Gaussian-beam into the substrate lens, the Gaussicity can also be thought of as a measure of the aberrations introduced by the lens. For extension lengths up to the hyperhemispherical position the Gaussicity is close to 100%. This is expected since the hyperhemispherical lens is aplanatic, implying the absence of spherical aberrations, and satisfies the sine condition, which guarantees the absence of circular coma [5]. As the extension length increases past  $R/n$ , the Gaussicity continuously decreases, which implies the introduction of more and more aberrations. In addition, the reflection loss typically increases after the hyperhemispherical extension length (depending on the beamwidth of the feed antenna). The total power coupling into the antenna, termed the Gaussian-coupling efficiency, is the product of the Gaussicity and all losses (reflection loss, dielectric loss, backside loss, etc.). This implies that the Gaussian-coupling efficiency decreases after the hyperhemispherical extension length ( $R/n$ ). Calculations in [1] and [3] indicate that for an intermediate position between the hyperhemispherical and diffraction-limited extension lengths, the Gaussian-coupling efficiency decreases by a small amount ( $< 10\%$ ), while the directivity is close to that of the diffraction-limited case.

If the substrate lens is to be used with an imaging array, it is necessary to characterize its off-axis performance (Fig. 1). A ray-optics/field-integration formulation similar to that described in [2] is used to solve for the radiation patterns and Gaussian-coupling efficiencies.

## II. THEORETICAL CALCULATIONS

The resulting scan angle for a displacement off-axis ( $D/R$ , where  $D$  is the distance off-axis and  $R$  is the radius of the lens) is shown in Figure 2 at three different extension lengths

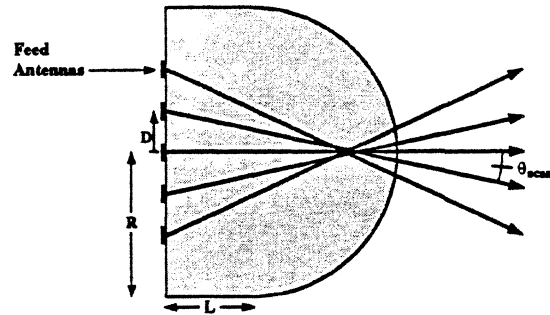


Figure 1: Imaging Array on Extended Hemispherical Lens

( $L/R$ , where  $L$  is the extension length): hyperhemispherical, intermediate, and synth. ellipse (diffraction-limited position), and for both silicon ( $\epsilon_r=11.7$ ) and quartz ( $\epsilon_r=3.8$ ) dielectric lenses. As expected, for a given  $D/R$  off-axis, a silicon dielectric lens will have a larger scan angle than the quartz lens due to its higher dielectric constant. Also, note that the off-axis positions are not dependent on the wavelengths away from the center, but on the percentage of the lens radius.

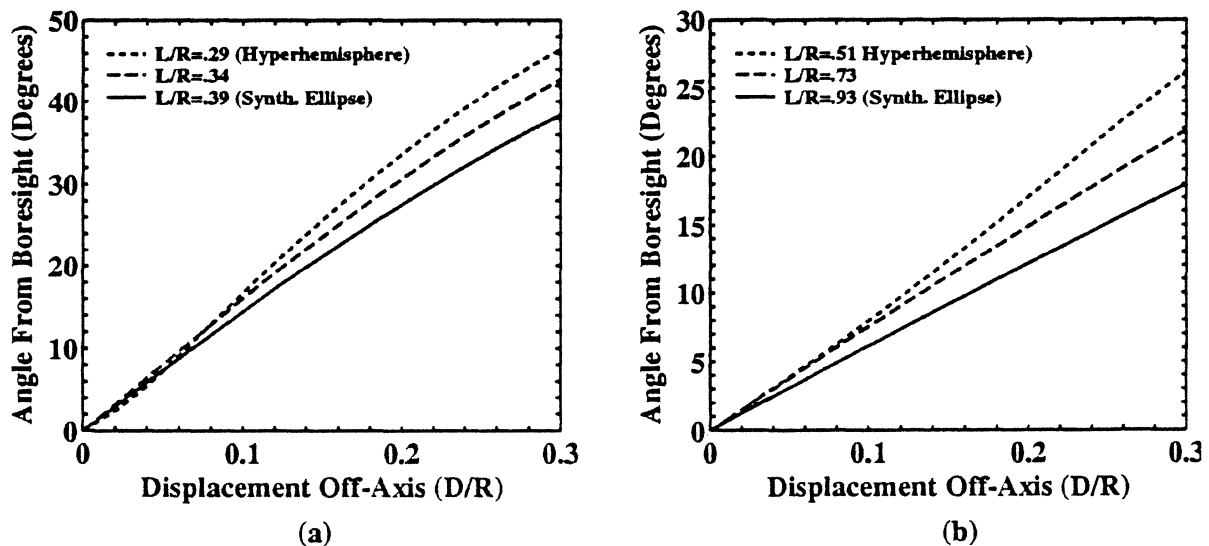


Figure 2: Scan angle versus off-axis displacement at fixed extension lengths for a silicon (a) and a quartz (b) lens.

The effect of an off-axis displacement in the H-plane at the hyperhemispherical po-

sition ( $L/R=0.29$ ) for a  $12\lambda$ -diameter silicon lens is shown in Figure 3. It is interesting to see that the patterns become sharper, and achieve a maximum directivity of 29.6dB at  $D/R=0.24$ , after which the directivity begins to slowly decrease. Therefore diffraction-limited performance can be nearly achieved by either increasing the extension length on-axis past the hyperhemispherical position, or by moving the feed antenna position off-axis in the hyperhemispherical plane. This can best be seen by the directivity contour plots for silicon and quartz in Figure 4. Note that moving off-axis does not achieve the full diffraction limited performance possible, and in the case of the silicon lens in the hyperhemispherical plane, it is 1.2dB lower than the maximum possible on-axis directivity of 30.8dB at  $L/R=0.38$ .

Figure 5 shows the maximum Gaussicity plots for a  $12\lambda$ -diameter silicon and quartz lens. To calculate the maximum Gaussicity, the Gaussian-beam waist and radius of curvature are optimized for each displacement off-axis. In addition, the phase center (the point through which the axis of the Gaussian-beam lies) is also changed to optimize the beam, however nearly the same result will be achieved if the phase center is assumed to be about  $0.4R$  behind the tip of the lens (see Fig. 1). Note for off-axis displacements, that the Gaussicity drops the most in the hyperhemispherical plane and the least for the synthesized elliptical plane. In fact, for a  $12\lambda$ -diameter quartz lens, the Gaussicity is a nearly constant 85% for off-axis displacements in the synthesized elliptical plane. Similar characteristics are observed in a  $24\lambda$ -diameter silicon and quartz lens, and is shown in Figure 6. However, for the larger lens the decreases in Gaussicity are magnified (for the same reasons as explained in [1]).

To calculate the Gaussian-coupling efficiency it is necessary to know the reflection loss in addition to the Gaussicity. The reflection loss for silicon and quartz lenses (independent of frequency or physical lens radius) is shown in Figure 7 for off-axis displacements. Note that the reflection losses rapidly increase for a silicon lens after  $D/R=0.1$ , while quartz lenses can be used to  $D/R=0.25$  with less than a 1dB increase in reflection loss. These curves are expected to be about 1.5dB lower for a silicon lens and 0.65dB lower for a quartz lens with a matching-cap layer.

### III. EXPERIMENTAL RESULTS: PATTERNS

A three element linear array of double-slot antennas was fabricated and measured on a silicon substrate lens at 258GHz [6]. The lens radius is 6.858mm and the extension length is chosen to be  $L=2.20\text{mm}$ . The double-slot antenna design is similar to that in [1], but with integrated Schottky diodes replacing the bolometers. The slot antennas are chosen to be  $0.30\lambda_0$ -long ( $354\mu\text{m}$ ) with a separation of  $0.16\lambda_0$  ( $190\mu\text{m}$ ) where  $\lambda_0$  is the free-space wavelength at 258GHz. The central antenna element is aligned to the center of the substrate lens, while the other two elements are  $800\mu\text{m}$  and  $1600\mu\text{m}$  off-axis in the H-Plane, respectively. The measured and theoretical H-plane patterns are shown in Figure 8. The agreement is quite good, predicting the scanned angle and even the -17dB sidelobe of the  $800\mu\text{m}$  off-axis pattern. The deviation between experimental and theoretical patterns at the  $1600\mu\text{m}$  off-axis position is most likely due to lens blockage and/or mount reflections at extreme angles.

### IV. CONCLUSION

The well-known hyperhemispherical position ( $R/n$ ) has the least aberrations and the best Gaussian-coupling efficiency. However, we have demonstrated that the hyperhemispherical plane is not the best extension length for imaging applications, since the directivity increases (and beamwidth decreases) by large values (9dB for a  $12\lambda$ -diameter silicon lens) for off-axis displacements. For high off-axis Gaussian-coupling efficiencies, this would necessitate the use of narrower Gaussian-beams off-axis, an impossible consideration since most optical systems utilize nearly fixed beam parameters. It was found for different types of lenses, that an extension length just before the synthesized elliptical position maintains the directivity and the Gaussian-beam parameters the most constant.

## REFERENCES

- [1] D.F. Filipovic, S.S. Gearhart and G.M. Rebeiz, "Double slot antennas on extended hemispherical and elliptical silicon dielectric lenses," *IEEE Trans. on Microwave Theory Tech.*, vol. 41, pp. 1738-1749, October 1991.
- [2] T.H. Büttgenbach, "An improved solution for integrated array optics in quasi-optical millimeter and submillimeter waves receivers: the hybrid antenna," *IEEE Trans. on Microwave Theory Tech.*, vol. 41, pp. 1750-1761, October 1991.
- [3] D.F. Filipovic and G.M. Rebeiz, "Double slot antennas on extended hemispherical and elliptical quartz dielectric lenses," *Int. J. Infrared Millimeter Waves*, vol. 14, pp. 1905-1924, October 1991.
- [4] G.V. Eleftheriades, "Double slot antennas on extended silicon lenses-general treatment," *University of Michigan Radiation Laboratory Report RL903*, February 1994.
- [5] M. Born and E. Wolf, *Principles of Optics*. New York: Permagon Press, pp. 252-252, 1959.
- [6] S.S. Gearhart and G.M. Rebeiz, "A monolithic 250GHz Shottky-diode receiver," to appear in the 1994 IEEE-MTT Symposium Issue, December 1994.

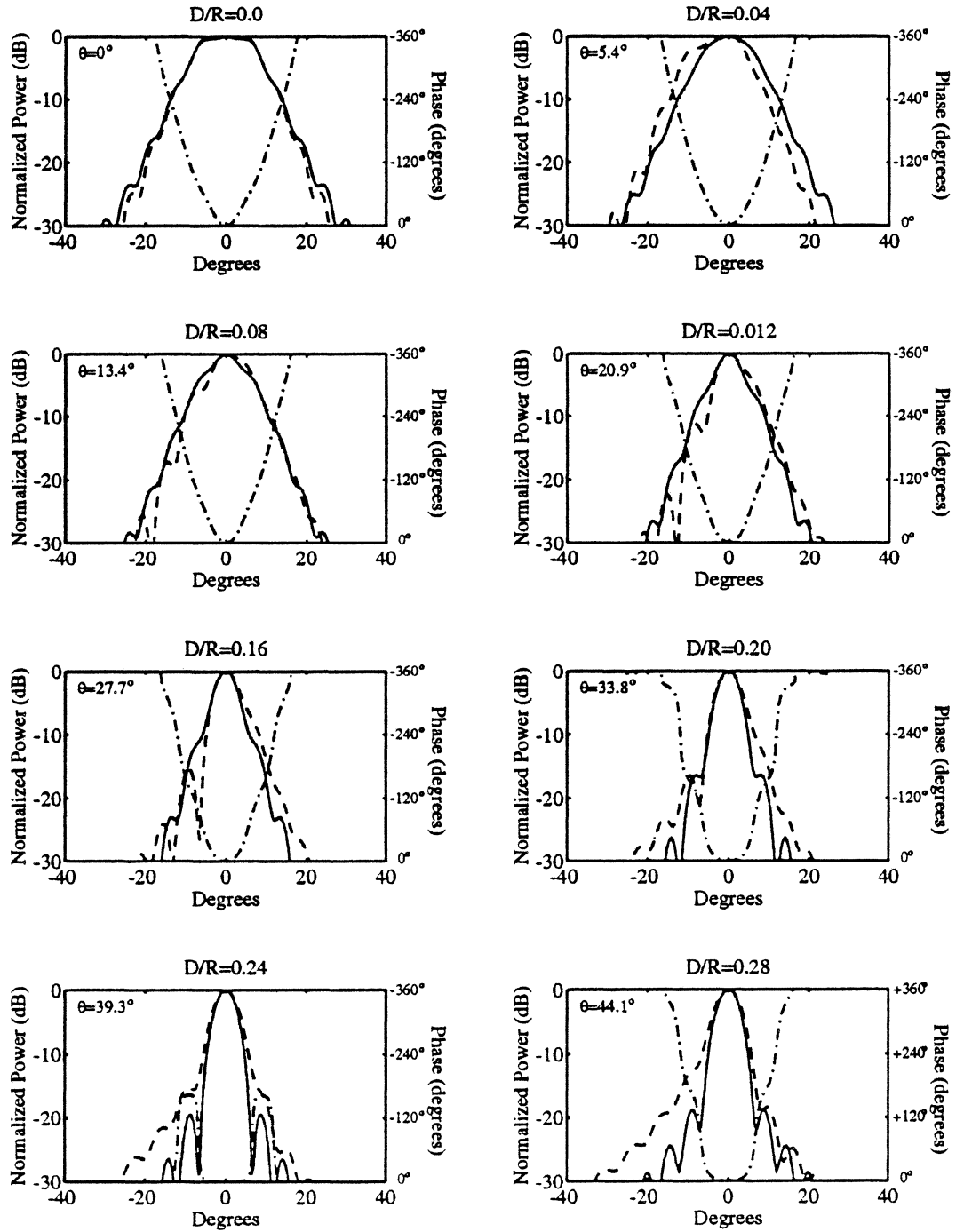


Figure 3: E and H-plane power patterns and H-plane phase for off-axis displacements in the H-plane at the hyperhemispherical extension length ( $L/R=0.29$ ) for a  $12\lambda$ -diameter silicon lens. The dashed/dotted line corresponds to the phase.

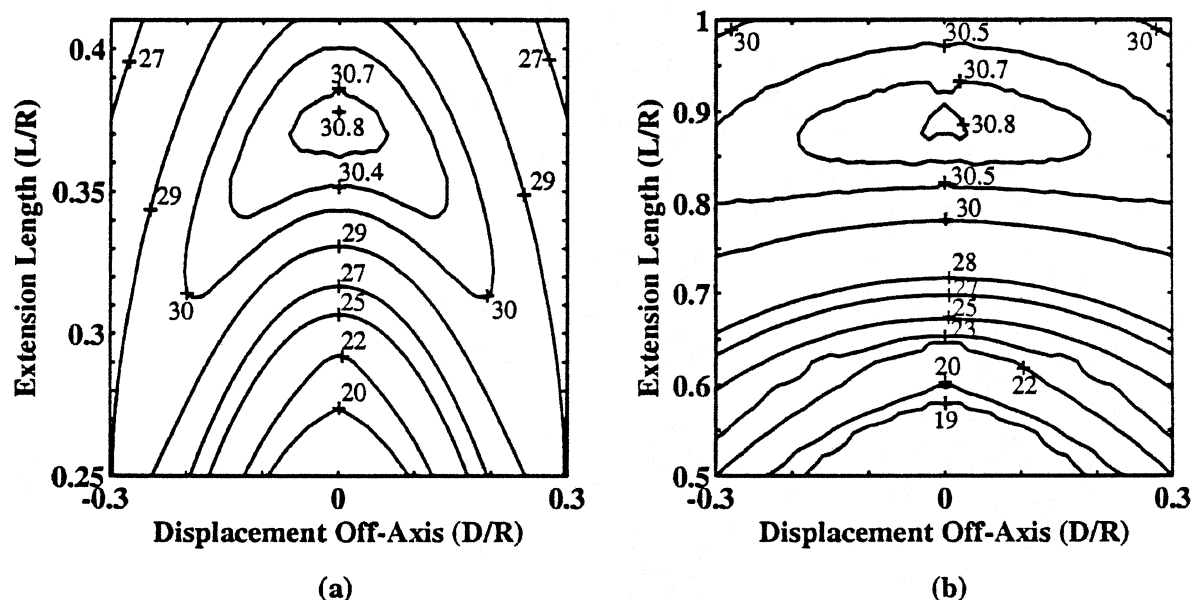


Figure 4: Directivity contour plots of silicon (a) and quartz (b) versus extension length and off-axis displacement.

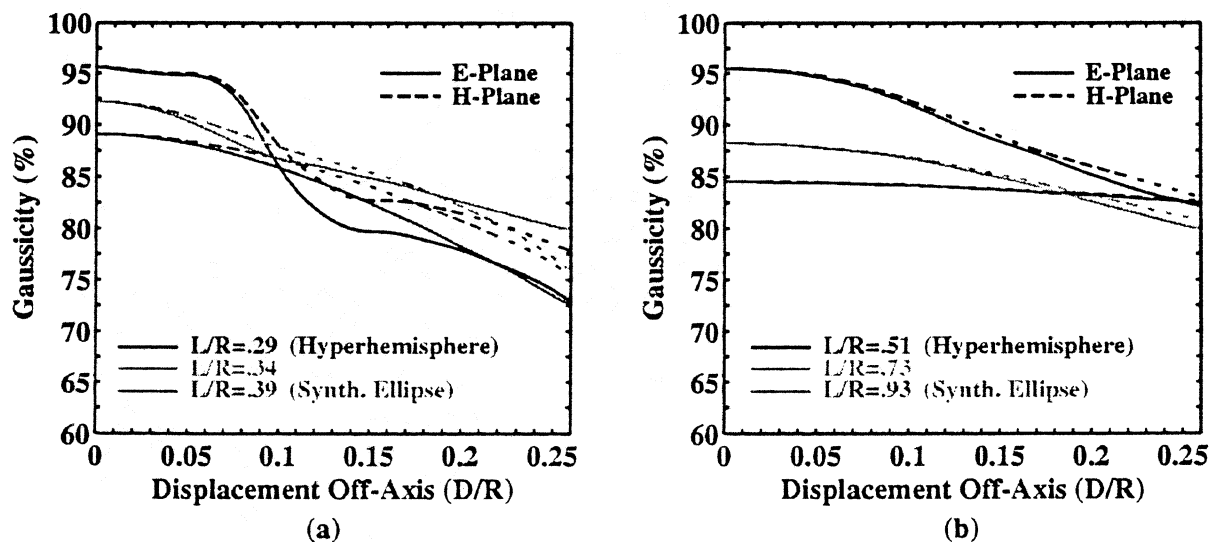


Figure 5: Gaussicity versus off-axis displacement at fixed extension lengths for a  $12\lambda$ -diameter silicon (a) and quartz (b) lens.



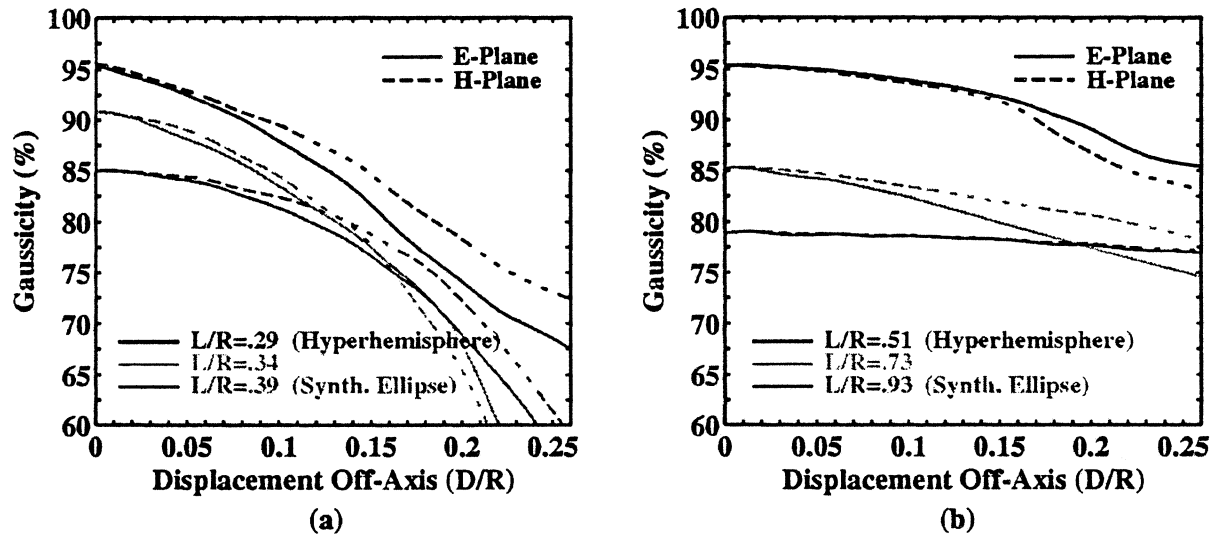


Figure 6: Gaussicity versus off-axis displacement at fixed extension lengths for a  $24\lambda$ -diameter silicon (a) and quartz (b) lens.

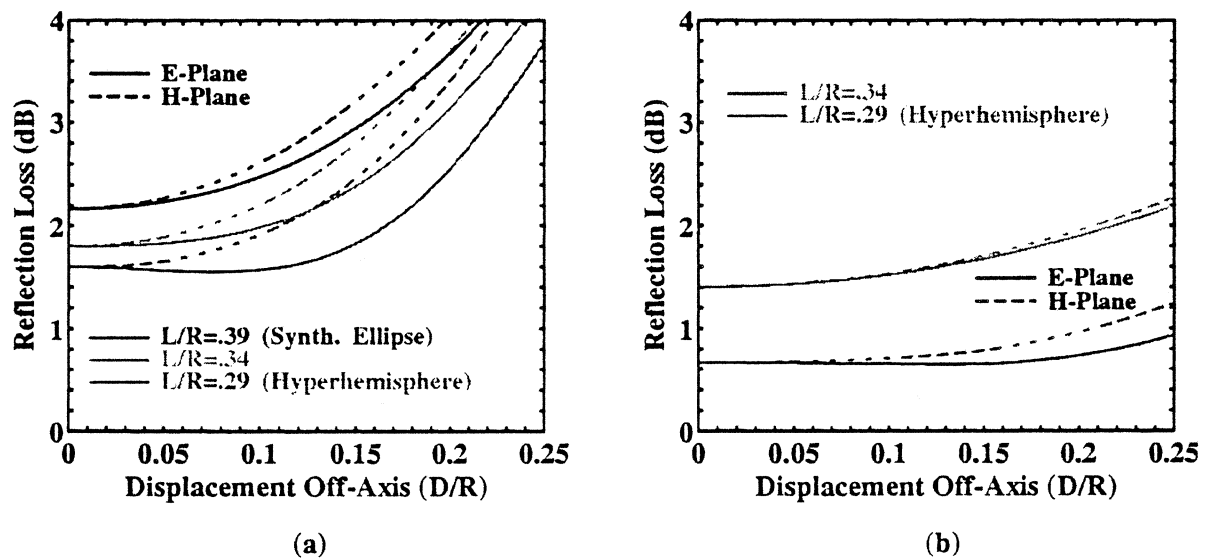


Figure 7: Reflection loss versus off-axis displacement at fixed extension lengths for a silicon (a) and quartz (b) lens.

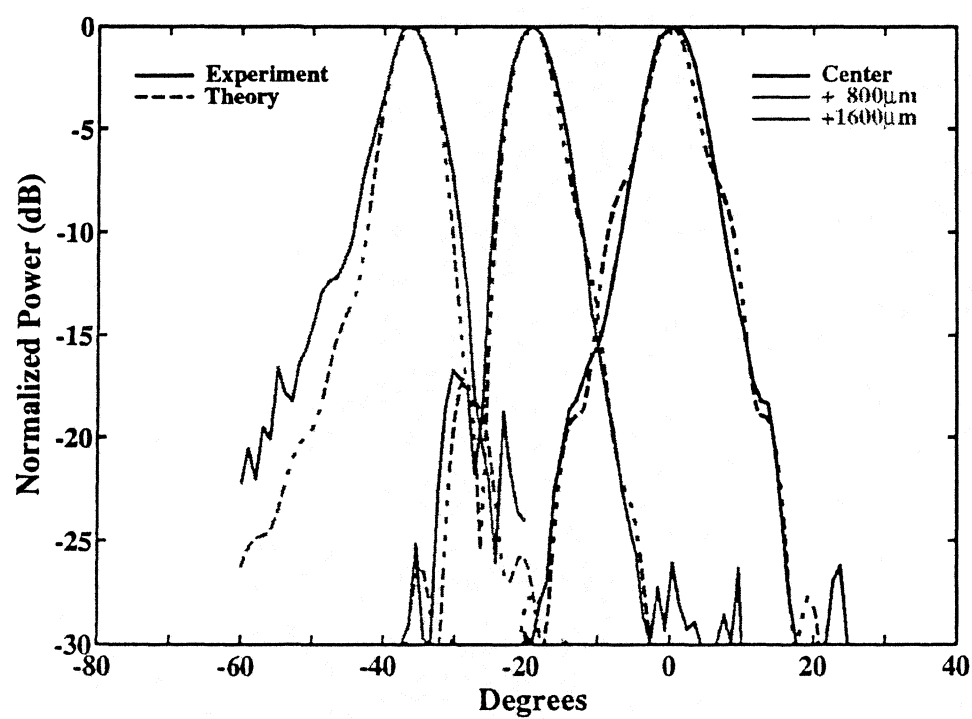


Figure 8: Comparison of theoretical and measured H-plane patterns at 258GHz.